Research article

Maize Sciences, 2026, xx: 100015

Exploration of QTLs for Resistance to *Fusarium* Ear Rot in Maize

Jing WEN[1], Mingxia JIN[2], Yidan LI[1], Kexing GUAN[1], Mo ZHU[1], Jiale DONG[1], Hongxia HE[1], Nan LI[1], Yuexian XING[3,#], Yan ZHANG[1,#]

([1]*Jilin Provincial Key Laboratory of Agricultural Biotechnology, Institute of Agricultural Biotechnology, Jilin Academy of Agricultural Sciences (Northeast Agricultural Research Center of China), Changchun 130033, China;* [2]*Lishu County Agricultural Comprehensive Law Enforcement Brigade, Lishu 136000, China;* [3]*Maize Research Institute, Jilin Academy of Agricultural Sciences (Northeast Agricultural Research Center of China), Gongzhuling 136100, China;* [#]*These authors contributed equally as co-corresponding authors*)

Abstract: Maize ear rot is a fungal disease that poses a serious threat to maize production. Many different pathogens can cause this disease, and one of the most frequently found is *Fusarium verticillioides*, which causes *Fusarium* ear rot (FER). To explore quantitative trait loci (QTLs) controlling FER resistance, a mapping population consisting of 158 F_2 individuals along with their $F_{2:3}$ families was developed from a cross of the resistant inbred line K10 with the susceptible inbred line ZW18. The two parental lines and the 158 $F_{2:3}$ families were grown in the field, inoculated, and scored for disease severity. The estimated broad-sense heritability (H^2) of FER resistance reached 0.78, which suggested that genetic factors were the main contributors to the phenotypic variation. Five QTLs for FER resistance were identified in total, accounting for 6.57%–38.24% of the phenotypic variation, and four of these QTLs were consistently detected in more than one replication. The FER resistance QTLs found in this work may serve as promising targets for improving maize FER resistance by transferring them into susceptible inbred lines through marker-assisted selection.

Key words: ear rot; *Fusarium verticillioides*; exploration; quantitative trait locus

INTRODUCTION

Ear rot is a fungal disease that seriously threatens maize production. It not only directly causes ear rot and yield reduction, but the toxins produced by its pathogens also harm human and animal health and food safety (Wang et al., 2011). In recent years, affected by factors such as global climate change, continuous cropping, straw return to the field, and high-water and high-fertilizer cultivation patterns, the occurrence of maize ear rot in China has intensified year by year: in severe years, the incidence rate can reach 30%–40%, the incidence rate of susceptible varieties can be as high as 50%, annual yield losses generally exceed 10%, and in heavily affected areas can reach more than 30% (Duan et al., 2020). It has become a biotic stress factor that seriously restricts the sustainable development of the maize industry. In particular, against the background of the increasing popularity of fully mechanized maize harvesting, the grain direct-harvest model makes it difficult to remove diseased ears during harvest, making the disease resistance of the varieties themselves increasingly important. Currently, chemical agents and cultivation measures are mainly adopted for the prevention and control of ear rot in maize, but the effects are limited. In comparison, breeding and promoting disease-resistant varieties is the most economical and effective approach.

The pathogens causing maize ear rot are diverse, and *Fusarium verticillioides*, the causal agent of *Fusarium* ear rot (FER), is among the most common. When FER occurs, a white mold layer is usually formed on maize kernels. Introgression of resistance genes/quantitative trait loci (QTLs) from donors into elite maize germplasm would be a feasible approach to develop resistant germplasm and commercial hybrids. For FER, researchers have made progress in QTL mapping, associated locus mining, and resistance gene cloning through linkage analysis, genome-wide association study (GWAS), transcriptome sequencing, and other approaches. Pérez-Brito et al. (2001) mapped nine and seven FER

Received: 8 October 2026; **Accepted:** 27 October 2026
Corresponding authors: Yuexian Xing (E-mail: xingyuexianzy@163.com); Yan Zhang (E-mail: zhangyan4023@163.com)
©The Author(s) 2026. Published by Higher Education Press
This is an open access article under the CC BY license (http://creativecommons.org/licenses/by/4.0)
https://doi.org/10.2738/MS.2026.0015

resistance QTLs in two $F_{2:3}$ populations, respectively, among which 3 QTLs could be detected in both populations. Using 187 recombinant inbred lines, two common FER resistance QTLs were detected under different environments, among which the major QTL explained 13%–22% of the phenotypic variation (Ding et al., 2008). Li et al. (2011) mapped four FER resistance QTLs on chromosomes 3, 4, 5, and 6, each explaining 2.5%–10.2% of the phenotypic variation. Using three F_2 populations and their corresponding $F_{2:3}$ families, a total of 20 FER resistance QTLs were mapped, six of which shared overlapping intervals (Wen et al., 2020). Xia et al. (2022) mapped 17 resistance QTLs significantly associated with FER, among which *qFER1.03* was fine-mapped to 0.2 Mb and explained 3.88%–15.62% of the phenotypic variation. In addition, some studies have reported FER resistance QTLs (Neupane et al., 2025; Butrón et al., 2019; Coan et al., 2018; Ju et al., 2017; Maschietto et al., 2017).

GWAS was also used to mine resistance-associated loci. In 2013, Zila et al. (2013) detected three associated SNP loci through GWAS, which together explained 3%–10% of the phenotypic variation, and the genes corresponding to two SNP loci were functionally related to programmed cell death. In 2018, 12 molecular markers associated with FER resistance were detected, and the gene corresponding to one locus was an NBS-LRR-type receptor (Jong et al., 2018); in 2020, Yao et al. (2020) identified 69 genes potentially associated with FER resistance using GWAS, and transcriptome sequencing analysis further showed that most differentially expressed genes between resistant and susceptible materials were enriched in metabolic pathways such as plant hormone signal transduction, phenylalanine metabolism, and cytochrome P450. Ayesiga et al. (2024) identified seven SNP loci associated with FER resistance, explaining 4%–11% of the phenotypic variation, and identified seven metabolic pathways related to FER resistance. Additionally, there are other reports on the identification of loci associated with FER resistance (Wu et al., 2020; Liu et al., 2021). In terms of resistance gene cloning, *ZmAuxRP1* is, to date, the only cloned FER resistance gene, which encodes an auxin-related regulatory protein and exhibits quantitative resistance to Gibberella stalk rot and FER, reflecting the important role of auxin signaling in broad-spectrum disease resistance (Ye et al., 2019).

Although many QTLs and candidate genes have been reported, most genes or loci exhibit minor effects on FER resistance in maize. This indicates that pyramiding of QTLs/genes from different sources would be an effective approach to improve FER resistance. Therefore, more effective QTLs need to be identified to provide resources for molecular breeding of FER resistance in maize. In this study, QTL mapping was conducted using an F_2 population and its corresponding $F_{2:3}$ families developed by crossing a highly FER-resistant inbred line with a susceptible inbred line. In addition, a high-resolution genetic linkage map was constructed, which can be used to identify markers for cloning QTLs or to introduce QTLs via marker-assisted selection (MAS), thereby improving maize resistance to FER.

RESULTS

Phenotypic analysis and broad-sense heritability (H^2) estimation

To identify QTLs conferring FER resistance in maize, both parents and the $F_{2:3}$ families derived from the F_2 population were artificially inoculated with *Fusarium verticillioides*, and disease severity was then scored. Disease severity was scored in two experimental replications in 2025 and another two in 2026. The mean disease severity score of each $F_{2:3}$ family was used as the phenotypic value of the corresponding F_2 individual. The results showed that in the two 2025 replications (2025_Rep1 and 2025_Rep2), the FER severity scores of the resistant parent K10 were 1.00 and 1.73, respectively, whereas those of the susceptible parent ZW18 were 6.25 and 5.75. In the two 2026 replications (2026_Rep1 and 2026_Rep2), the FER disease severity scores were 1.00 and 1.18 for K10, and 6.20 and 7.00 for ZW18. Across the four replications in two years, the resistant parent K10 maintained stable resistance across environments, while the susceptible parent ZW18 showed a consistent susceptible response (Fig. 1). In the F_2 segregating population, FER severity did not show a bimodal distribution (Fig. 2), suggesting that this trait is not controlled by a single major gene but may be jointly regulated by multiple QTLs.

Skewness tests showed that among the four replications (2025_Rep1, 2025_Rep2, 2026_Rep1, and 2026_Rep2), only the FER severity of the F_2 population in 2025_Rep1 was normally distributed, while the other three were not (Fig. 2; Table 1). By contrast, the residuals were all normally distributed (Fig. 3; Table 1).

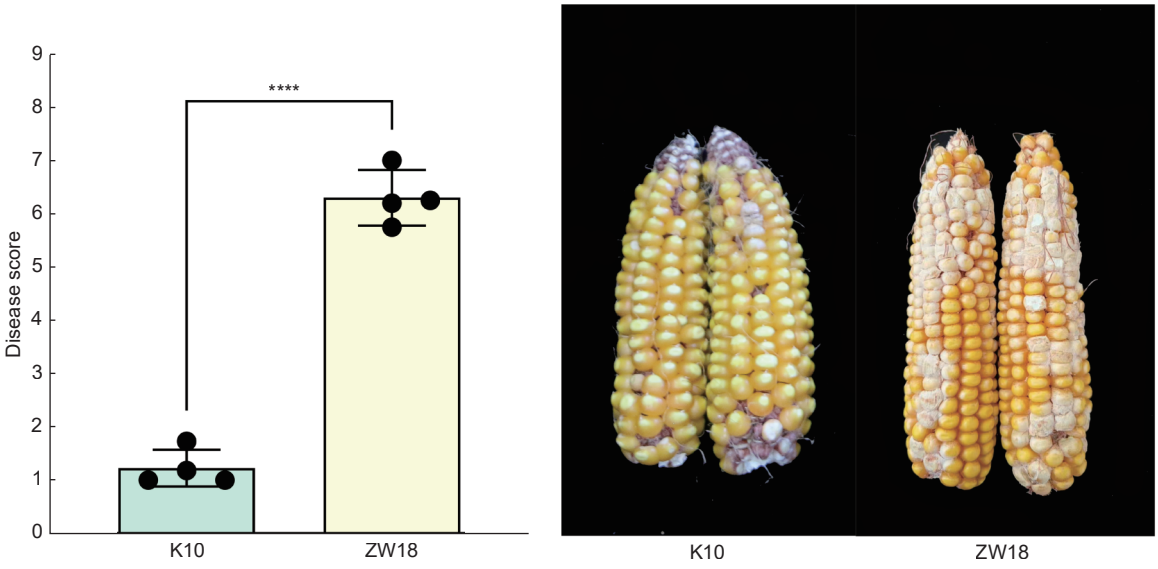


Fig. 1. Comparison of FER severity between parental inbred lines.

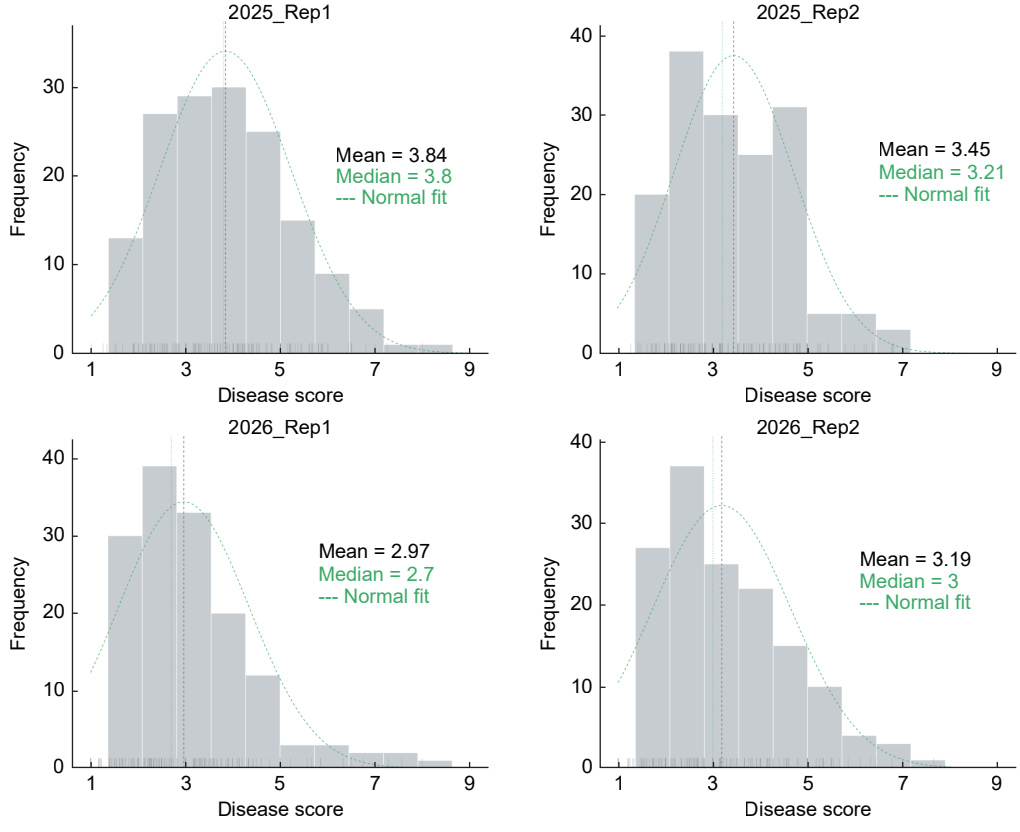


Fig. 2. Frequency distribution of FER severity in the F_2 population.

Therefore, the phenotypic data from all four replications could be used for QTL mapping of resistance. Analysis of variance (ANOVA) based on the phenotypic data from each replication of the F_2 population showed that FER resistance differed significantly among genotypes and between years, whereas interaction effects between genotype and environment were not significant (Table 2). Furthermore, the broad-sense heritability (H^2) of FER resistance was estimated using multiple replication phenotypes of the F_2 population, yielding a value of 0.78.

Construction of the genetic linkage map

An F_2 population generated from a cross between the

Table 1. Phenotypic analysis of FER severity of parents and F_2 population.

Replication	Resistant parents	Susceptible parents	F_2 population					
			Mean	SD	Skewness	Kurtosis	Shapiro-Wilk test *P* value	Shapiro-Wilk test *P* value of residuals
2025_Rep1	1.00	6.25	3.84	1.39	0.36	−0.39	0.05	0.98
2025_Rep2	1.73	5.75	3.45	1.26	0.52	−0.42	1.63×10^{-4}	0.85
2026_Rep1	1.00	6.20	2.97	1.38	1.10	1.51	3.40×10^{-7}	0.97
2026_Rep2	1.18	7.00	3.19	1.46	0.67	−0.09	0.74×10^{-4}	0.85

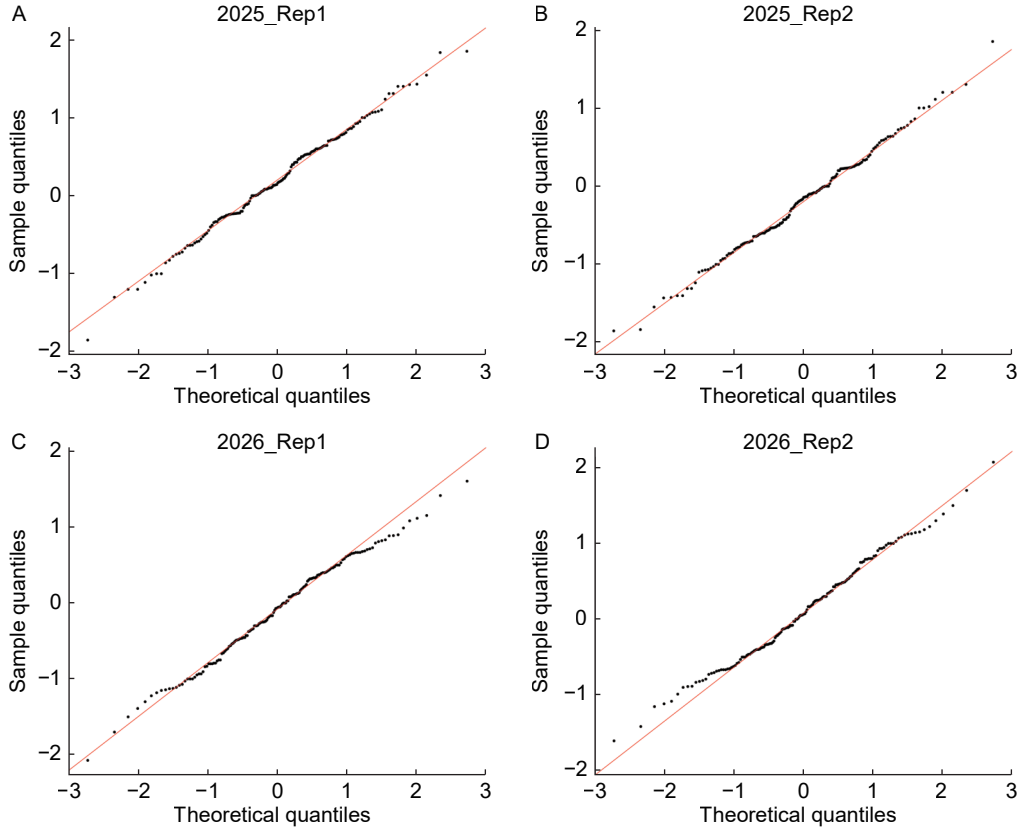


Fig. 3. Quantile–quantile (Q–Q) plot of FER severity residual in F_2 population.

Table 2. Analysis of variance for FER severity of F_2 population.

Sources	Df	SS	MS	*F* value	*P* value	Significance
G	157	738.77	4.71	5.06	2.20×10^{-16}	***
Y	1	51.27	51.27	55.15	1.05×10^{-12}	***
G:Y	157	165.35	1.05	1.13	0.18	
Residuals	315	292.83	0.93			

G: Genotype; Y: Year; G:Y: Interaction between genotype and environment.

parental lines K10 and ZW18 was used to construct a genetic linkage map. From a total of 11 535 raw molecular markers, 4301 SNP markers that were polymorphic between the two parents were selected. After further removing 1249 markers showing segregation distortion, 3052 high-quality SNP markers were retained for map construction. Using the "MAP" module in QTL IciMapping software (version 4.2), a genetic map containing 10 linkage groups was successfully constructed (Fig. 4). The total genetic

length of the map was 2589.8 cM (Table 3), and the average genetic distance between adjacent markers was 0.85 cM. The markers were relatively evenly distributed across the linkage groups (Fig. 4), indicating that the constructed map is suitable for subsequent QTL mapping analysis.

QTL mapping for FER resistance

QTL mapping for FER resistance in maize was performed using phenotypic data from four replications (2025_Rep1, 2025_Rep2, 2026_Rep1, and 2026_Rep2) and across two years (2025 and 2026), together with the best linear unbiased estimator (BLUE) value calculated from the phenotypic data of four replications in the F_2 population. A total of five FER-resistant QTLs were detected—*qRferK2.1*, *qRferK4.1*, *qRferK7.1*, *qRferK7.2*, and *qRferK7.3*—with explained phenotypic variation ranging from 6.57% to 38.24% (Fig. 5, Table 4). All five FER-resistant QTLs derived from the resistant parent K10, four of which could be detected in more than one replication.

qRferK2.1, which was located in bins 2.01–2.02, was mapped using phenotypic data from 2025 and the BLUE value, explaining 13.86%–17.05% of the phenotypic variation (Fig. 5, Table 4). Based on phenotypic data from 2025_Rep2, 2026_Rep1, 2025, 2026, and the BLUE value, *qRferK4.1* was identified, which was located in bins 4.06–4.07 and accounted for 10.88%–38.24% of the phenotypic variation (Fig. 5, Table 4). For *qRferK7.1* in bins 7.01–7.02, detection was achieved using the 2025_Rep2 phenotype, explaining 6.57% of the phenotypic variation (Fig. 5, Table 4). *qRferK7.2*, which was

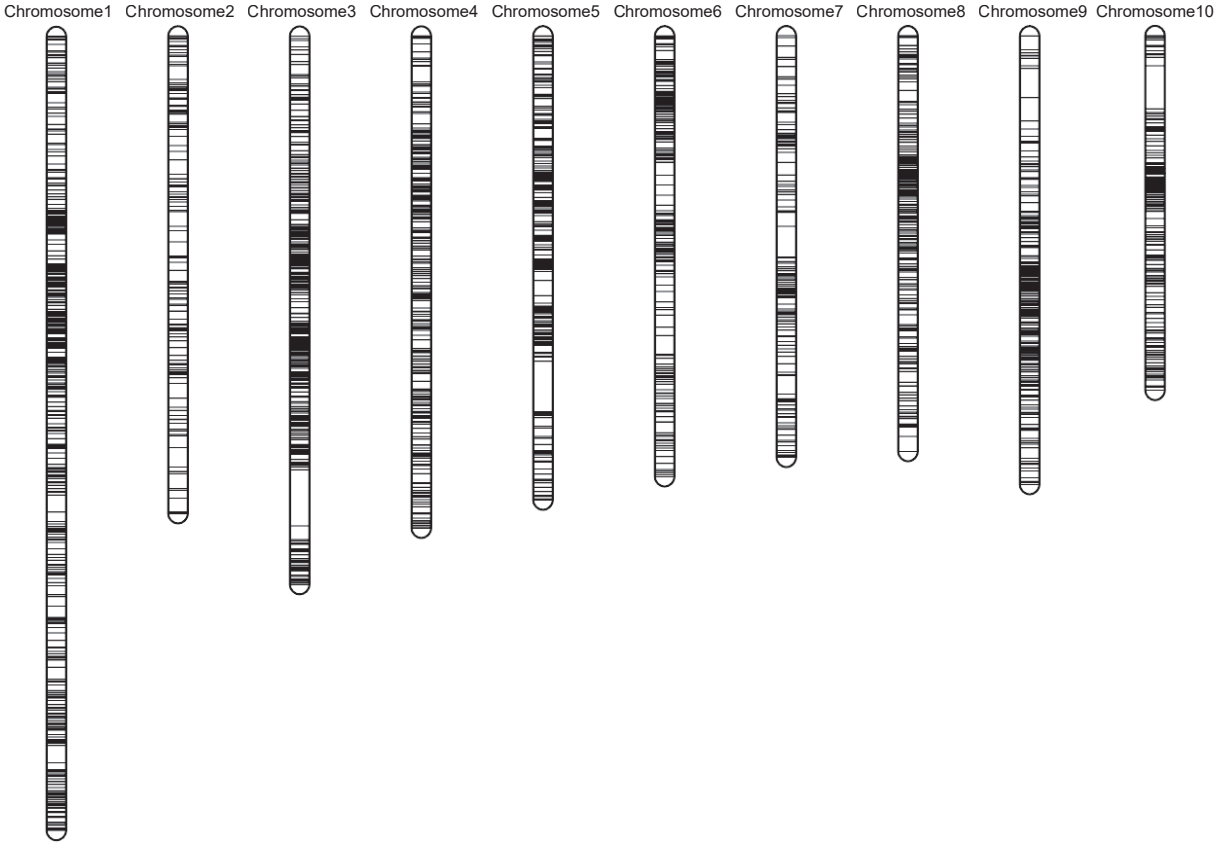


Fig. 4. Genetic linkage map constructed based on the F_2 mapping population.

Table 3. Length and number of markers for each linkage group of the constructed linkage map.

Parameter	Linkage groups										Average	Total
	1	2	3	4	5	6	7	8	9	10		
Length（cM）	418.0	255.0	291.0	262.1	247.8	235.6	226.0	223.0	240.0	191.3	259.0	2589.8
No. of markers	555	163	428	410	314	248	169	253	287	225	305	3052

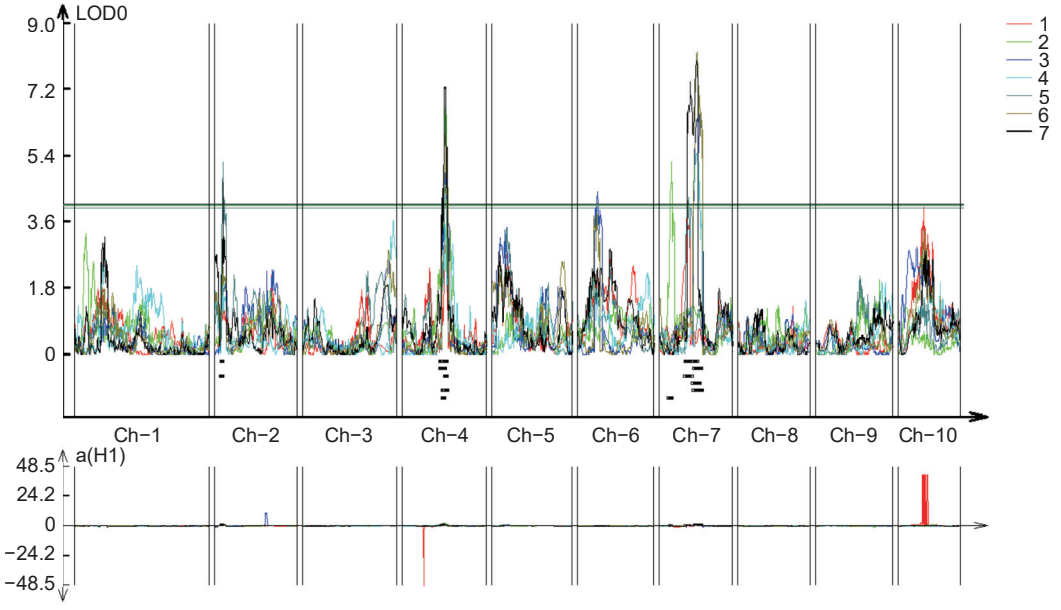


Fig. 5. Detection of FER resistance QTLs in F_2 population.
1: 2025_Rep1; 2: 2025_Rep2; 3: 2026_Rep1; 4: 2026_Rep2; 5: 2025; 6: 2026; 7: BLUE.

Table 4. Parameters associated with quantitative trait loci (QTLs) for FER resistance.

QTL	Chromosome	Bins	Replication	Confidence interval	LOD	LOD peak marker	Additive	Dominant	SRA	R^2(%)
qRferK2.1	2	2.01-2.02	2025	2_3703096-2_8868897	5.23	2_6475800	0.63	−0.29	K10	17.05
	2	2.01-2.02	BLUE	2_3703096-2_8868897	4.69	2_6475800	0.74	−0.18	K10	13.86
qRferK4.1	4	4.06-4.07	2025_Rep2	4_170368406-4_178525271	6.93	4_176007875	1.32	−0.41	K10	38.24
	4	4.06-4.07	2026_Rep1	4_170368406-4_179648042	4.96	4_175369292	0.64	−0.11	K10	11.78
	4	4.06-4.07	2025	4_170368406-4_178525271	4.03	4_177683436	0.49	−0.16	K10	10.88
	4	4.06-4.07	2026	4_170368406-4_179648042	5.97	4_175369292	0.64	−0.11	K10	13.96
	4	4.06-4.07	BLUE	4_170368406-4_178525271	7.26	4_175369292	0.59	−0.29	K10	19.80
qRferK7.1	7	7.01-7.02	2025_Rep2	7_4554422-7_16676992	5.23	7_6132578	0.61	0.26	K10	6.57
qRferK7.2	7	7.02	2025	7_115113886-7_124984565	4.29	7_118460634	0.51	−0.04	K10	9.42
	7	7.02	BLUE	7_115751731-7_124984565	7.42	7_120590962	0.64	0.13	K10	10.79
qRferK7.3	7	7.02-7.03	2026_Rep1	7_124984565-7_145337837	6.43	7_134132654	0.83	−0.12	K10	18.20
	7	7.02-7.03	2026_Rep2	7_124984565-7_138407644	5.49	7_134132654	0.86	−0.09	K10	15.84
	7	7.02-7.03	2026	7_124984565-7_143145895	8.24	7_134132654	0.88	−0.33	K10	31.26
	7	7.02-7.03	BLUE	7_124984565-7_137653512	7.99	7_134132654	0.74	−0.09	K10	22.01

R^2: percentage of phenotypic variation explained by the QTL; SRA: source of resistance allele; Marker name consists of the chromosome number and physical position (based on the B73 RefGen_v3 assembly), separated by a hyphen.

detected in bin 7.02 using phenotypic data from 2025 and the BLUE value, accounted for 9.42%–10.79% of the phenotypic variation (Fig. 5, Table 4). *qRferK7.3*, located in bins 7.02–7.03, was detected from phenotypic data of 2026_Rep1, 2026_Rep2, 2026, and the BLUE value, accounting for 15.84%–31.26% of the phenotypic variation (Fig. 5, Table 4). In addition, the FER resistance conferred by all five mapped QTLs exhibited both additive and dominant effects, although additive effects were predominant

(Table 4).

DISCUSSION

Obtaining objective and maximally accurate disease phenotypic data is the most critical step in this study, and also the most challenging task. The core technical difficulty lies in the fact that, due to differences in the flowering periods of different materials, if inoculation is performed at the same time, the differences in grain development stages caused by the different flowering periods of each material will lead to differences in their resistance to infection at different developmental stages, thereby introducing considerable experimental error. To circumvent this problem, all plants in this study were open-pollinated, and each material was manually inoculated with a spore suspension of the pathogen on the 12th day after its own silking, so as to ensure that pathogen infection occurred at a stage when grain development was essentially consistent across all materials. Although this procedure prolongs the duration of manual inoculation work and may introduce certain experimental error due to subtle differences in the inoculation environment among materials, such error is far smaller than that caused by inconsistent grain developmental progression. In terms of disease evaluation, this study adopted a scoring method based on estimation of the diseased area, which may produce some bias due to subjective factors. However, because there are substantial resistance differences between the resistant and susceptible parents themselves, and the disease phenotypes in the segregating population also show pronounced differentiation, the error caused by subjective factors does not substantially affect subsequent QTL mapping work. In addition, in the field of disease evaluation, researchers have recently developed more precise automated analysis systems, providing new technical solutions for high-throughput phenotyping of maize ear rot (Yao et al., 2026). Subsequent studies will refer to the latest research findings and attempt to improve the current disease evaluation system of this study.

In resistance QTL mapping studies, the existence of significant resistance differences between resistant and susceptible parents is a prerequisite for conducting mapping work. In this study, the resistant parent K10 exhibited stable high resistance to FER (mean disease severity score of 1.23), whereas the susceptible parent ZW18 was stably susceptible (mean disease severity score of 6.30). Therefore, the use of these two inbred lines to construct a segregating population for mapping QTLs conferring FER resistance in maize is reasonable and relatively ideal in terms of applicability. In previous studies, joint mapping using three populations identified resistance QTLs in bins 1.03, 1.04–1.07, 2.04–2.08, 4.05–4.08, 6.03–6.06, and 7.01–7.02 across different resistance sources, suggesting that these overlapping regions may represent potential resistance “hotspots” (Wen et al., 2020). In the present study, *qRferK4.1* and *qRferK7.1* both reside within the aforementioned “hotspot” regions. Specifically, the mapping interval of *qRferK4.1* completely overlaps with those of the previously mapped *qRfer3*, *qRfer8*, and *qRfer18*, and the mapping interval of *qRferK7.1* completely overlaps with that of the previously mapped *qRfer10* and partially overlaps with that of *qRfer4*. These results further reinforce the reliability of the six “hotspot” regions previously identified.

Previous reports have indicated that FER resistance is inherited as a quantitative trait, with both additive and dominant effects (Zhou et al., 2021). In this study, the broad-sense heritability of FER resistance was estimated to be as high as 0.78, indicating that FER resistance is inherited as a quantitative trait. Furthermore, all five resistance QTLs detected in this study exhibited both additive and dominant effects, but were predominantly governed by additive effects. In addition, the sum of the dominant effects of all mapped QTLs was negative, indicating that individuals carrying heterozygous genotypes within the target QTL intervals are more likely to exhibit FER resistance.

In recent years, the incidence and severity of maize ear rot have been increasing year by year. Meanwhile, with the acceleration of full-process mechanization in maize production, the grain direct-harvesting model cannot effectively remove diseased ears during the harvesting stage, so that the intrinsic resistance of varieties has become the primary line of defense against ear rot damage. However, since it was first reported in 1987 that the predominant pathogen of maize ear rot in China was *Fusarium verticillioides*, numerous subsequent identifications of maize ear rot pathogens have consistently shown that *Fusarium verticillioides* remains the dominant pathogen of maize ear rot in China (Pan et al., 1987). This fact indicates that, over a long period, the varieties deployed in maize production in China have

consistently lacked resistance to *Fusarium verticillioides*. Therefore, there is an urgent need to clone resistance genes and to breed and promote resistant varieties. Over the past two decades, researchers have mapped a number of FER resistance QTLs on different maize chromosomes through linkage analysis and genome-wide association studies. However, most of these QTLs have only small effects, and cloning genes conferring FER resistance has progressed slowly because of complex genetic mechanisms. To date, resistance QTLs or genes that can be stably inherited and directly applied in breeding have rarely been reported, and the regulatory network of resistance genes remains unclear. Therefore, continuing to mine more stable resistance QTLs and achieving the transition from "mapping QTLs" to "cloning major genes and dissecting resistance mechanisms" represent the core tasks and current developmental trends. This study provides a preliminary approach for such genetic analyses.

MATERIALS AND METHODS

Plant materials

A mapping population of 158 F_2 individuals and their corresponding $F_{2:3}$ families was derived from a cross between the FER-resistant inbred line K10 and the susceptible inbred line ZW18 to map FER resistance QTLs.

Pathogen culture and artificial inoculation

The *Fusarium verticillioides* strain was cultured on potato dextrose agar (PDA) plates at 25 °C in the dark for approximately 7 days. After the mycelia had fully covered the plates, the cultures were stored at 4 °C for later use. Prior to inoculation, each medium plate with pathogen was cut into 1 cm^2 pieces and transferred into 1000 mL of 5% mung bean broth liquid medium, followed by incubation at 25 °C on a rotary shaker at 150 r/min for 3 days. After incubation, the mycelial mats were removed by filtration, and the conidial suspension was collected and stored at 4 °C. One day before inoculation, the conidial concentration was adjusted to 5×10^6 conidia·mL^{-1} with sterile distilled water, and the surfactant Tween-80 was added to a final concentration of 2 μL·mL^{-1}. At 12 days after silking, 2 mL of conidial suspension was injected into the middle of each maize ear with a syringe.

FER disease evaluation and phenotypic analysis

The parental inbred lines and the 158 $F_{2:3}$ families were planted for field inoculation and disease evaluation in the spring of 2025 and 2026 at the Gongzhuling Experimental Station, Jilin Province. The experiment was arranged in a randomized block design with two replications (blocks) per year and four replications in total across the two years. Each block contained the 158 $F_{2:3}$ families and the two parental inbred lines. Each entry was planted in a single row per replication, with a row length of 5 m, row spacing of 0.6 m, and plant spacing of 0.25 m (21 plants per row). The survival rate of all plots was above 90%, and all surviving plants were artificially inoculated and scored for disease severity. At 30 days after inoculation, the severity of FER was scored using a 5-grade scale (1, 3, 5, 7, and 9), corresponding to the following infected area percentages: grade 1 (0%–2%), grade 3 (3%–10%), grade 5 (11%–25%), grade 7 (26%–50%), and grade 9 (51%–100%). The field management was identical in both years. The temperature from mid-July to early August in 2026 was higher than that in 2025, while the other climatic conditions were basically the same.

After FER disease evaluation, phenotypic data were analyzed by ANOVA using R software, based on the model $Y = \mu + \alpha_G + \beta_Y + (\alpha\beta)_{GY} + \varepsilon_{GYR}$, where α_G represented the effect of Gth line, β_Y was the effect of the Yth year, $(\alpha\beta)_{GY}$ was the effect of the genotype by year interaction, and ε_{GYR} was the residual effect. Variance components were estimated using the lme4 package in R. Broad-sense heritability was calculated from the estimated variance components as $H^2 = \sigma^2_G/(\sigma^2_G + \sigma^2_{GY}/R + \sigma^2_e/YR)$ (Knapp et al., 1985), where σ^2_G was the genetic variance, σ^2_{GY} was an interaction variance of genotype by year, σ^2_e was the residual error, R was the number of replications per year, and Y was the number of years. Based on the decomposition of variance components, the mean square (MS) for G can be decomposed as $\sigma^2_e + R\sigma^2_{GY} + RY\sigma^2_G$, the MS for Y as $\sigma^2_e + R\sigma^2_{GY} + RG\sigma^2_Y$, the MS for $G{:}Y$ as $\sigma^2_e + R\sigma^2_{GY}$, and the *residual* MS as σ^2_e. From these, σ^2_G, σ^2_{GY}, and σ^2_e can be estimated separately, allowing the broad-sense heritability to be calculated.

Genotyping and construction of linkage maps

Young leaves of the parental inbred lines and the F_2 population were collected at the 5–6 leaf stage for

genomic DNA extraction. Genotyping of each individual was performed using the GenoBaits Maize10K chip based on the Genotyping by Target Sequencing (GBTS) platform. Then SNP markers showing polymorphism between the two parents were selected from the raw genotype data, and markers with significant segregation distortion ($P < 0.05$) were removed. A linkage map was constructed using the "MAP" module of QTL IciMapping software (version 4.2) (Meng et al., 2015). Linkage groups were defined with a LOD threshold, and recombination frequencies were converted into genetic distances (cM) using the Kosambi mapping function.

QTL detection for resistance to FER

The mean phenotypic values of each $F_{2:3}$ family were used as the phenotypic values of the corresponding F_2 individual. Combined with the genetic linkage data and phenotypic data from the F_2 population, QTL mapping for resistance to FER in maize was performed using the composite interval mapping (CIM) method implemented in QTL Cartographer software (version 2.5) (Zeng, 1994; Basten et al., 1997), based on phenotypic data of four replications (2025_Rep1, 2025_Rep2, 2026_Rep1, 2026_Rep2) and two years (average value of two corresponding replications, represented accordingly as 2025 and 2026), as well as the BLUE value calculated from the phenotypic data of four replications. In the CIM analysis, Model 6 (Standard Model) was selected, with a walk speed of 1.0 cM and a window size of 10.0 cM, so that markers within 10 cM on either side of the tested position were excluded as cofactors to avoid masking the signal of the target interval. A maximum of five background markers were used as cofactors, which were selected by backward regression from the genome-wide markers and dynamically chosen within the Model 6 framework according to the specified marker number and window size to control background genetic effects. The LOD significance threshold was determined automatically by the software through a permutation test (1000 permutations, significance level 0.05).

ACKNOWLEDGEMENTS

This study was funded by Science and Technology Development Plan Project of Jilin Province, China (20260101046JJ) and Basic Research Fund Project of Jilin Academy of Agricultural Sciences (Northeast Agricultural Research Center of China) (KYJF2025JJ011).

DATA AVAILABILITY

Data are available from the corresponding author upon reasonable request.

DECLARATION OF COMPETING INTEREST

The authors declare no competing interests.

REFERENCES

Ayesiga S B, Rubaihayo P, Oloka B M, et al. 2024. Genome-wide association study and pathway analysis to decipher loci associated with *Fusarium* ear rot resistance in tropical maize germplasm. *Genetic Resources and Crop Evolution*, **71**: 2435−2448.

Basten C J, Weir B S, Zeng Z B. 1997. QTL Cartographer: A reference manual and tutorial for QTL mapping. Department of Statistics, North Carolina State University, Raleigh, NC.

Butrón A, Santiago R, Cao A, et al. 2019. QTLs for resistance to *Fusarium* ear rot in a multiparent advanced generation intercross (MAGIC) maize population. *Plant Disease*, **103**: 897−904.

Coan M M D, Senhorinho H J C, Pinto R J B, et al. 2018. Genome-wide association study of resistance to ear rot by *Fusarium verticillioides* in a tropical field maize and popcorn core collection. *Crop Science*, **58**: 564−578.

Ding J Q, Wang X M, Chander S, et al. 2008. QTL mapping of resistance to *Fusarium* ear rot using a RIL population in maize. *Molecular Breeding*, **22**: 395−403.

Duan C X, Wang B B, Sun F F, et al. 2020. Occurrence of maize ear rot caused by *Fusarium fujikuroi* in China. *Plant Disease*, **104**: 587.

Jong G D, Pamplona A K A, Pinho R G V, et al. 2018. Genome-wide association analysis of ear rot resistance caused by *Fusarium verticillioides* in maize. *Genomics*, **110**: 291−303.

Ju M, Zhou Z J, Mu C, et al. 2017. Dissecting the genetic architecture of *Fusarium verticillioides* seed rot resistance in maize by combining QTL mapping and genome-wide association analysis. *Scientific Reports*, **7**: 46446.

Knapp S J, Stroup W W, Ross W M. 1985. Exact confidence intervals for heritability on a progeny mean basis. *Crop Science*, **25**: 192−194.

Li Z M, Ding J Q, Wang R X, et al. 2011. A new QTL for resistance to *Fusarium* ear rot in maize. *Journal of Applied Genetics*, **52**: 403−406.

Liu Y B, Hu G H, Zhang A, et al. 2021. Genome-wide association study and genomic prediction of *Fusarium* ear rot resistance in tropical maize germplasm. *The Crop Journal*, **9**: 325−341.

Maschietto V, Colombi C, Pirona R, et al. 2017. QTL mapping and candidate genes for resistance to *Fusarium* ear rot and fumonisin contamination in maize. *BMC Plant Biology*, **17**(20): 20.

Meng L, Li H H, Zhang L Y, et al. 2015. QTL IciMapping: Integrated software for genetic linkage map construction and quantitative trait locus mapping in biparental populations. *The Crop Journal*, **3**(3): 269−283.

Neupane S P, Stagnati L, Dell'Acqua M, et al. 2025. Genetic basis of *Fusarium* ear rot resistance and productivity traits in a heterozygous multi-parent recombinant inbred intercross (RIX) maize population. *BMC Plant Biology*, **25**: 639.

Pan H K, Zhang L X. 1987. Resistance of maize to the *Fusarium* ear-rot pathogen. *Acta Agriculturae Boreali-Sinica*, **2**: 86−89.

Pérez-Brito D, Jeffers D, González-De-León D, et al. 2001. QTL mapping of *Fusarium moniliforme* ear rot resistance in highland maize, Mexico. *Agrociencia*, **35**: 181−196.

Wang J H, Ndoye M, Zhang J B, et al. 2011. Population structure and genetic diversity of the *Fusarium graminearum* species complex. *Toxins*, **3**: 1020−1037.

Wen J, Shen Y Q, Xing Y X, et al. 2020. QTL mapping of *Fusarium* ear rot resistance in maize. *Plant Disease*, **105**: 558−565.

Wu Y B, Zhou Z J, Dong C P, et al. 2020. Linkage mapping and genome-wide association study reveals conservative QTL and candidate genes for *Fusarium* rot resistance in maize. *BMC Genomics*, **21**: 357.

Xia Y S, Wang B B, Zhu L H, et al. 2022. Identification of a *Fusarium* ear rot resistance gene in maize by QTL mapping and RNA sequencing. *Frontiers in Plant Science*, **13**: 954546.

Yao L S, Li Y M, Ma C Y, et al. 2020. Combined genome-wide association study and transcriptome analysis reveal candidate genes for resistance to *Fusarium* ear rot in maize. *Journal of Integrative Plant Biology*, **62**: 1535−1551.

Yao X Y, Li X N, Zhang S Y, et al. 2026. Accurate detection of full-surface ear rot in maize using hyperspectral imaging and deep learning. *Food Research International*, **240**: 119658.

Ye J R, Zhong T, Zhang D F, et al. 2019. The auxin-regulated protein *ZmAuxRP1* coordinates the balance between root growth and stalk rot disease resistance in maize. *Molecular Plant*, **12**(3): 360−373.

Zeng Z B. 1994. Precision mapping of quantitative trait loci. *Genetics*, **136**: 1457−1468.

Zhou G F, Li S F, Ma L, et al. 2021. Mapping and validation of a stable quantitative trait locus conferring maize resistance to Gibberella ear rot. *Plant Disease*, **105**: 1984−1991.

Zila C T, Samayoa L F, Santiago R, et al. 2013. A genome-wide association study reveals genes associated with *Fusarium* ear rot resistance in a maize core diversity panel. *G3: Genes, Genomes, Genetics*, **3**: 2095−2104.